

## **ADSORPTIVE REMEDIATION OF ANILINE USING GRAPHITE: RESPONSE SURFACE METHODOLOGY AND PRINCIPAL COMPONENT ANALYSIS**

Chuan Xian Tan<sup>1</sup>, Voon-Loong Wong<sup>1,\*</sup>, Sue Jiun Phang<sup>1</sup>, Swee Pin Yeap<sup>2,3</sup>, Siew Shee Lim<sup>4</sup>

<sup>1</sup>School of Engineering and Physical Sciences, Heriot-Watt University Malaysia Campus, 62200, Wilayah Persekutuan Putrajaya, Malaysia.

<sup>2</sup>Department of Chemical and Petroleum Engineering, Faculty of Engineering, Technology & Built Environment, UCSI University, Kuala Lumpur, Malaysia.

<sup>3</sup>UCSI-Cheras Low Carbon Innovation Hub Research Consortium, Kuala Lumpur, Malaysia.

<sup>4</sup>Department of Chemical and Environmental Engineering, Faculty of Science and Engineering, University of Nottingham Malaysia, Jalan Broga, 43500 Semenyih, Selangor, Malaysia

\* Corresponding Author: [v.wong@hw.ac.uk](mailto:v.wong@hw.ac.uk) Tel: (+60) 3 8894 3788

---

**Abstract:** The effectiveness of graphite in aniline removal through adsorption was studied in batch mode based on four parameters: pH (3 to 11), temperature (30 to 50°C), initial aniline concentration (5 to 25 ppm) and graphite dosage (0.5 to 2.5 g). Box-Behnken design was adopted to build 27 experiments and investigated the manipulated parameters. Highest removal efficiency (95%) of aniline was achieved for 15 ppm solution at temperature of 40 °C and pH 3 using 1.5 g of graphite. Confirmation studies was conducted to evaluate the regression model's reliability. Principal Component Analysis (PCA) was used to explore the significant experimental variables and spot the outliers. Based on the research outcome, graphite can be feasible for aniline removal as it requires simple processing and available richly in nature.

Keywords: Adsorption; Graphite; Aniline; Optimization; Box-Behnken Design

---

### **1. Introduction**

Aniline, an organic chemical raw material that is widely used in pharmaceutical industry, agrochemical manufacture and material sciences (Deng, Chen, & Lei, 2018). The global consumption of aniline is increasing tremendously at an average annual rate of 3.2%, reaching more than 6.8 million metric tons in the year of 2021 (Markit, 2016). Excessive usage of aniline

has not only led to the accumulation of aniline compound in the wastewater effluent but also in the surface and ground water. Moreover, aniline is a threat to human health that particularly affects the upper respiratory tract due to its high toxicity. Hence, strategies to remove aniline has gained much attention from the public and researchers to remediate its adverse impact on human and environment. However, aniline is difficult to be removed owing to its stable component; moreover, aniline is readily adsorbed by the sediments, consequently becoming a permanent pollutant in the aquatic environment. Therefore, further investigations are required on the removal method to reduce the negative impact of aniline to human and environment (Li, Xu, & Yan, 2016).

Biological treatments (Jiang, Wang, Yu, & Yang, 2016), oxidation processes (Mohamed A., Mohamed F., Safinaz H., & Ahmed M., 2020), absorption (Coban, Biyik, & Saglam, 2020) and adsorption (Xiao, Zhou, Mao, & Wang, 2015) are the treatment procedures applied widely in the industry. Biological treatment of aniline effluent is conducted by growing specific bacteria population that has the ability to degrade aniline, and biological treatment is commonly applied for large volume treatment. Nevertheless, this treatment method is relatively time consuming as the bacteria which is highly sensitive to surrounding conditions must be cultivated (Wang, Barrington, & Kim, 2007).

Advanced oxidation process (AOPs) is another common aniline degradation method. AOP has been widely employed for the degradation of harmful organic pollutants, mainly with the use of hydroxyl radical derivatives during industrial effluent treatment (Anotai, Su, Tsai, & Lu, 2011) (Jin, Lee, Chang, Huang, & Swaminathan, 2006). Particularly, Fenton process is one of the AOPs that involves catalytic reaction between ferrous ion and hydrogen peroxide to generate hydroxyl radicals for wastewater treatment (Anotai, Su, Tsai, & Lu, 2010). Fenton process has several distinct advantages, which include low capital cost and simple operations. However, the process generates a huge quantity of ferric hydroxide sludge which in turn requires further treatment before disposal to the environment (Anotai, Su, Tsai, & Lu, 2010). Therefore, it limits the implementation of Fenton process in wastewater treatment and further researches are required to increase the practicality of this technique.

Besides AOPs, adsorption is another alternative approach for the removal of aniline. Adsorption has been regarded as an advantageous procedure for pollutant removal, especially for the ones with low concentration due to its low cost and high efficiency (Deng, Chen, & Lei, 2018). In fact, numerous of adsorbents with different characteristics have been studied and recommended by several researchers (Liu, Zhang, & Huang, 2015) (Deng, Chen, & Lei, 2018)

(Verma, Thakur, Mamba, & Prateek, 2020). Selection of appropriate adsorbent is significant as different adsorbents possess different removal efficiency towards specific components. Activated carbon (Liu, Zhang, & Huang, 2015), graphene oxide (Deng, Chen, & Lei, 2018), metal-organic framework materials (Chen, et al., 2017) and polymeric materials (Cai, et al., 2005) are few of the popular adsorbents in waste removal.

Activated carbon is an outstanding adsorbent ascribable to its high adsorption capacity and excellent resistance to abrasion. Nonetheless, the low dispersibility possessed by activated carbon powder limits its adsorption performance towards pollutant. One of the practices in enhancing dispersibility is to coat the activated carbon with biological materials (Liu, Zhang, & Huang, 2015). Apart from that, graphene oxide-modified attapulgite composite is another prominent adsorbent in aniline degradation. Graphene oxide (GO) is a compound with unique two-dimensional structure, featuring high surface area and abundant oxygen functional groups with excellent adsorption performance in aniline removal (Deng, Chen, & Lei, 2018). Nonetheless, the practical implementations of GO composites as an adsorbent are limited due to exorbitant cost of GO (Liu, et al., 2018).

In present work, graphite was selected as an alternative adsorbent and its effectiveness towards aniline removal was systematically assessed through process optimization using response surface methodology (RSM) and principal component analysis (PCA). Graphite is a 3D structure with layers of graphene sheet stacked together and it possesses attractive chemical properties, thermal stability, and mechanical strength. The fabrication process of graphite is comparatively simpler as compared to that of GO, where further oxidation of graphite oxide using intensive amount of solvent is required (Smith, LaChance, Zeng, Liu, & Sun, 2019). Hence, it has the potential to be an excellent adsorption material in waste removal process (Mah et al., 2023) (Verma, Thakur, Mamba, & Prateek, 2020).

## **2. Materials and Methods**

### **2.1 Materials**

Graphite powder (< 44 $\mu$ m; 99 %), aniline (99 %, MW: 93.13 g/mol), sodium hydroxide (99 %, MW: 39.99 g/mol) and hydrochloric acid (99 %, MW: 36.46 g/mol) were purchased from Sigma-Aldrich, Germany. Distilled water was used throughout the experiments. All chemical reagents were of analytical grade (AR) and applied without further purification.

## 2.2 Batch Adsorption Process

One hundred millilitres (100 mL) of 10 ppm aniline solution were prepared in a conical flask with its initial absorbance measured. An amount of 0.5 g fresh graphite powder was then added into the conical flask. Following that, the conical flask containing graphite-aniline suspension was transferred into the incubator shaker (IKA KS 4000 i control shakers, Malaysia) at 30 °C, 200 rpm for 6 hours. For each sample, three identical sets were prepared, and their absorbance measurements were averaged to ensure the accuracy of this study. The absorbance of each aniline solution was measured at 230 nm using the UV-Vis spectrophotometer (HACH DR6000, USA). Three millilitres (3 mL) of the sample were collected from each conical flask and centrifuged (Eppendorf Centrifuge 5430) at 10000 rpm for 3 mins to separate the graphite from aniline solution prior to its absorbance measurement. The absorbance of the aniline solution was measured at every 1-hr interval for a total duration of 6 hrs. The removal percentage of fresh graphite was calculated using equation (1) (Naga Babu, et al., 2017):

$$\text{Removal Percentage (R \%)} = \frac{C_0 - C_t}{C_0} \times 100\% \quad (1)$$

where R % is the aniline removal percentage (%),  $C_0$  is the initial concentration of aniline solution (ppm), and  $C_t$  is the concentration of aniline solution at time t (ppm).

## 2.3 Response Surface Methodology (RSM)

In present study, Box-Behnken, a four independent variables fractional factorial design was chosen due to the fewer experimental sequences of the variables to evaluate potential complex response functions. The pH value of aniline solution, temperature of incubator shaker, initial aniline concentration and dosage of graphite were the four variables studied in the optimization study. Levels of the 4 different factors were shown in **Table 1** and were applied to generated experimental matrix using Design of Experiment (DOE) based on Box-Behnken experimental design under RSM in Minitab 19. A total of 27 sets experiments were required to justify the optimum conditions. Different dosage of graphite and 60 mL of aniline solutions with different pH and initial aniline solutions were put into 100 mL conical flask and swirled with an incubator shaker (IKA KS 4000 i control shakers, Malaysia) at 200 rpm and at different temperature range for 6 hours. The pH of dye solution was adjusted by adding either 0.05 M of NaOH or 0.05 M of HCl and measured by using a pH meter (Eutech pH 150, Singapore) before the graphite powder was added. The removal percentage was selected as the output objective function which was calculated by using Equation (1).

**Table 1.** Levels of the 4 different factors.

<b>Factors</b>	<b>Levels</b>		
<b>pH</b>	3	7	11
<b>Initial Aniline Concentration (ppm)</b>	5	15	25
<b>Dosage of Graphite (g)</b>	0.5	1.5	2.5
<b>Temperature of Incubator Shaker (°C)</b>	30	40	50

## 2.4 Regression Analysis and Confirmation Studies of Experiment

The experimental results from the 27 sets of optimisation experiments were computed into Minitab 19 to generate the regression equation with confidence level of 95% for all intervals. Stepwise of 0.15 was applied to maintain a hierarchical model to assure all the possible terms were shown in the model. Furthermore, a best-fit of transformation was generated by omitting the insignificant parameters which had P-value greater than 0.05 that results in an increase of the predicted proportion of variance,  $R^2$ . Therefore, the regression equation generated was used to calculate the predicted value for each variable. Confirmation of experiments was also carried out to examine the accuracy of regression equation generated from the regression analysis. The predicted values from the regression analysis were evaluated as well. Three sets of confirmation experiments under different experimental conditions were conducted and compared to the predicted values determined from the regression equation in previous section.

## 2.5 Multivariate Analysis: Principal Component Analysis (PCA)

The individual and combined influence of the variables on aniline adsorption using graphite was elucidated using PCA in present studies. The objective of the PCA analysis was to reduce the steps required for the machine learning algorithms to explore and visualize the outcome of the input (Jaadi, 2021). The first step for PCA was to determine the number of principal components and it can be done by looking at the proportion of variance that the components explain, eigenvalues and also scree plot. Subsequently, each principal component was interpreted by examining the magnitude and direction of the coefficients for the parameters.

## 3. Results and Discussion

### 3.1 Optimization Studies: Response Surface Methodology (RSM)

In **Table 2**, it was observed that set 14, 16 and 24 displayed the higher R% (> 90%) of aniline among other experimental runs. Therefore, the experimental conditions of each set-up were

reviewed to determine the optimal removal condition for aniline. The first parameter investigated was the pH value of the aniline solution, where the experiment was conducted at pH 3, pH 7 and pH 11. Based on the sets with highest R% of aniline, all 4 sets of experiments were carried out at pH 3, where large amount of H<sup>+</sup> ions were present in acidic condition. The deposition of H<sup>+</sup> ions on the graphite surface turned graphite into positively charge as the pH value is lower than its point of zero charge (PZC ~ pH 6.2) as shown in **Figure 1**. The positively charged graphite possessed high affinity towards aniline which was categorised as a weak anionic base (Deng, Chen, & Lei, 2018). In contrast, the adsorptive interaction between graphite and aniline was prohibited by electrostatic repulsion force at pH 11.

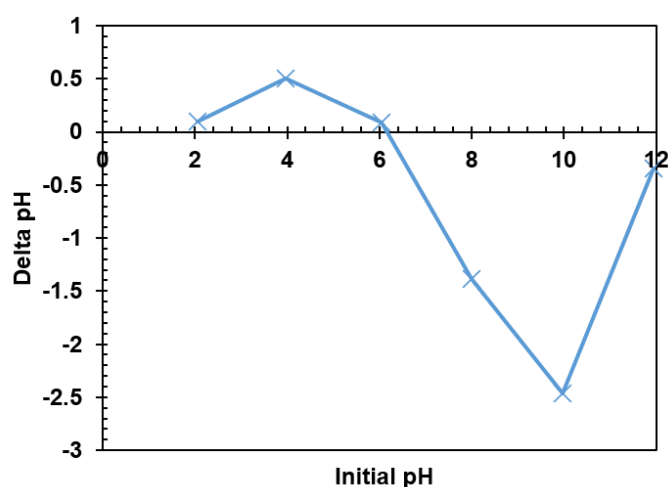


**Figure 1.** Zero-point measurement of graphite at different initial pH (temperature: 30°C; NaCl concentration: 0.01 M; dosage: 0.5 g).

The subsequent parameter was the initial aniline concentrations which were adjusted to 5 ppm, 15 ppm and 25 ppm in this study. Based on the 4 sets of experiments with highest R%, it observed that the optimum adsorption happened at 5 ppm and 15 ppm; 3 out of the 4 sets of experiments that have the highest R% were conducted at 15 ppm. Subsequently, 15 ppm was chosen as the optimal initial aniline concentration in this study as graphite was ineffective to remove a higher concentration (>15 ppm) of aniline due to limited adsorption capacity per one molecule of graphite (Oetjik & Ibrahim, 2021). Furthermore, the third parameter was the graphite dosage where 0.5 g, 1.0 g and 1.5 g were the dosages applied in the experiment. A higher R% of aniline was achieved as the graphite dosage increased, however, at dosage of 2.5 g, an increase in dosage led to a reduction in R% attributed to the excessive active sites, hence, 1.5 g of dosage was chosen (Padmavathy, Madhu, & Haseena, 2016). The medium temperature was studied in this adsorption procedures where the temperatures investigated were set at 30 °C, 40 °C and 50 °C. Based on the results, it showed that the medium temperature has least

impact towards the aniline adsorption as similar R% was observed even with a change in temperature.

**Table 2.** RSM results based on four experimental conditions.

Set	pH	Temperature (°C)	Initial Concentration (ppm)	Graphite Dosage (g)	R%
1	11	30	15	1.5	16.6
2	7	40	15	1.5	38.8
3	7	50	15	2.5	58.3
4	3	40	15	2.5	85.1
5	7	40	15	1.5	35.4
6	11	40	5	1.5	27.1
7	7	40	5	2.5	60.8
8	7	50	15	0.5	44.0
9	11	40	15	0.5	29.4
10	7	40	5	0.5	32.9
11	7	50	5	1.5	65.2
12	7	50	25	1.5	46.5
13	7	40	25	2.5	32.4
14	3	40	5	1.5	96.5
15	7	30	25	1.5	18.0
16	3	30	15	1.5	93.7
17	11	40	15	2.5	37.0
18	7	30	5	1.5	30.2
19	7	30	15	0.5	16.6
20	3	40	25	1.5	80.3
21	7	30	15	2.5	32.6
22	7	40	25	0.5	33.0
23	3	40	15	0.5	85.3
24	3	50	15	1.5	91.2
25	11	50	15	1.5	50.4
26	7	40	15	1.5	36.5
27	11	40	25	1.5	21.6

### 3.2 Regression Model

A second order regression equation was generated for aniline R% at using Minitab 19. The regression equation was shown in **Table 3**. Several statistics were included in the model summary table generated along the regression equation to justify the accuracy of the regression model. One of it was the S-value which served as an indicator of deviation for the input data from the fitted values. A minimum S-value revealed that the regression model has characterized the response well. In this scenario, the S-value obtained for 230 nm was 4.967 which represented that 95% of the data points were  $\pm 5\%$  from the fitted value. However, S-value should not be the sole indicator to prove that the regression model failed in satisfying the model assumptions. Thus, the residual plot was constructed to determine the consistency and reliability of the regression model.

**Table 3.** Model summary table for aniline removal regression model at  $\lambda_{\max}$  of 230 nm.

<b>R% (230 nm) = 153.6 - 34.55 pH - 0.357 Temperature +0.396 Initial Conc. +16.12 Dosage + 1.298 pH<sup>2</sup> + 0.2272 pH*Temperature - 0.714 Initial Conc.* Dosage</b>				
<b>S</b>	<b>R-sq</b>	<b>R-sq (adj)</b>	<b>PRESS</b>	<b>R-sq (pred)</b>
<b>4.967</b>	97.21%	96.18%	1126.59	93.30%

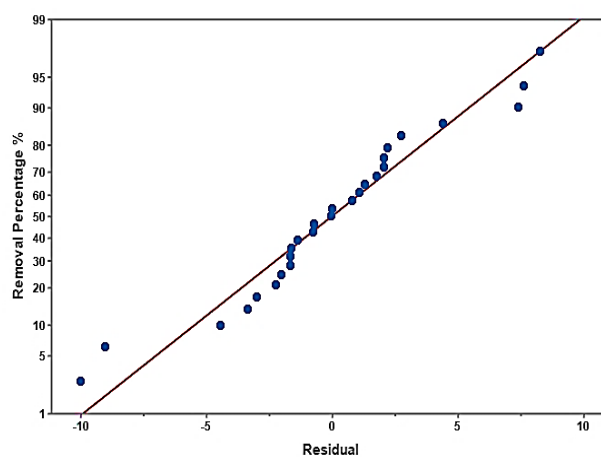


**Figure 2.** Normal probability plot for R% at 230nm.

Referring to **Figure 2**, the residual plot for R% at 230 nm displayed most of the residuals were well distributed, Therefore, the regression model generated satisfied the model assumptions. The adjusted R-sq value was 96.18% which proved that the predictors involved had significant impact. Moreover, the predicted R-sq value was applied to examine the over-fitting of the model. The predicted R-sq value was typically calculated using PRESS value where a low



PRESS value indicated that the model has a better predictive ability. A model with high R-sq value but low predicted R-sq value has the possibility of over-fitting. Based on the model summary table, the predicted R-sq value was 93.30%, validating that the model was not over-fitted.

### 3.3 Analysis of Variance (ANOVA) Results

The significance and contribution percentage of each combination was determined through ANOVA in Minitab 19. As presented in **Table 4**, contribution percentage, F- and P-value were listed accordingly. F-value was evaluated to determine the significance level of the parameters involved in the adsorption experiment and similarly used for the calculation of P-value. A high F-value implies that any changes of the particular parameter will have significant impact on the adsorption performance. Likewise, P-value was evaluated to determine the significance of respective parameter. A P-value of 0.05 or less indicated the parameter was significant to the adsorption performance and it was considered to be against the null hypothesis. Additionally, contribution percentage of each parameter or a combination thereof illustrated the capability of each parameter on explaining the response variability. A higher percentage indicated the parameter, or the combination of parameters was dominant in the response.

**Table 4.** ANOVA results for R% at wavelength of 230 nm.

Source	DF	Contribution	F-Value	P-Value
<b>Regression</b>	7	97.21%	94.63	0.000
<b>pH</b>	1	60.74%	130.76	0.000
<b>Temperature</b>	1	10.85%	0.61	0.445
<b>Initial Conc.</b>	1	3.25%	0.98	0.333
<b>Dosage</b>	1	2.09%	16.31	0.001
<b>pH<sup>2</sup></b>	1	17.10%	116.55	0.000
<b>pH*Temperature</b>	1	1.96%	13.39	0.002
<b>Initial Conc. *</b>	1	1.21%	8.27	0.010
<b>Dosage</b>				
<b>Error</b>	19	2.79%	-	-
<b>Total</b>	26	100.00%	-	-

Based on **Table 4**, it can be concluded that the medium temperature and aniline initial concentration were the least significant as the P-value for the respective parameter were larger

than 0.05. On the other hand, the medium pH was identified as the most significant parameter in aniline adsorption.

### 3.4 Deviation between Experimental Data and Predicted Value

The predicted values were determined using the regression model derived in section 3.2. The predicted values and experimental results were plotted as **Figure 3** (a) and (b). Based on **Figure 3** (a), the distribution of predicted values was well-distributed over the experimental data points. The deviation between the predicted values and experimental data for each set were plotted as in **Figure 3** (b) and the deviation is considerably negligible. A confirmation study was conducted to further evaluate the accuracy of the regression model using different experimental conditions.

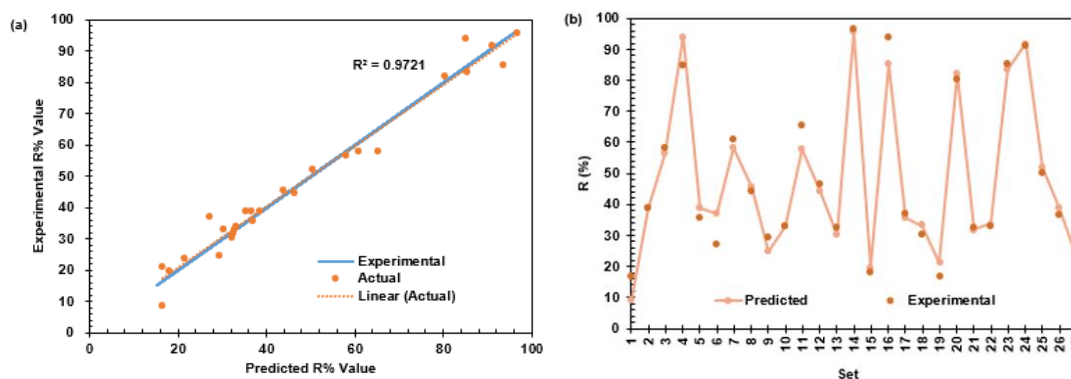


**Figure 3**

**Figure 3.** (a) Distribution of actual values over experimental data and (b) R% deviation between predicted value and experimental data for each set.

### 3.5 Confirmation of Experiments

**Table 5** listed on three sets of experimental conditions for respective confirmation experiment and its' predicted adsorptive performance results. Similar values were observed for both experimental data and predicted values for aniline removal at wavelength of 230 nm. Hence, the R% of aniline was well described by the regression equation generated with Minitab.

**Table 5.** Experimental conditions for confirmation studies.

Set	pH	Temperature (°C)	Initial Concentration (ppm)	Dosage of Graphite (g)	Experimental R%	Predicted R%
1	11	40	5	1	31.99	30.83
2	7	40	15	2.5	39.73	44.15

3      3      40      25      1.5      87.90      81.92

### 3.6 Multivariate Analysis: Principal Component Analysis

PCA was carried out to determine a smaller number of correlated variables, commonly known as the principal components from a large pool of data. The four manipulated variables and aniline R% at 6<sup>th</sup> hour were included as the analysis variables in present study. Based on the cumulative percentage in **Table 6**, it was shown that 77.5% of the variation is included in the first three principal components.

**Table 6.** Eigenanalysis of the correlation matrix at wavelength of 230 nm.

	PC1	PC2	PC3	PC4	PC5
<b>Eigenvalue</b>	1.877	1	1	1	0.1229
<b>Proportion</b>	0.375	0.2	0.2	0.2	0.025
<b>Cumulative</b>	0.375	0.575	<b>0.775</b>	0.975	1

**Table 7.** Eigenvectors at wavelength of 230 nm.

Variable	PC1	PC2	PC3	PC4	PC5
<b>pH</b>	<b>-0.628</b>	0.029	-0.327	0.321	-0.628
<b>Temperature</b>	0.266	0.318	<b>-0.86</b>	0.136	0.266
<b>Initial Conc.</b>	-0.145	<b>0.828</b>	0.136	-0.504	-0.145
<b>Dosage</b>	0.117	0.462	0.368	0.79	0.117
<b>R% (t=6 hr)</b>	<b>0.707</b>	0	0	0	-0.707

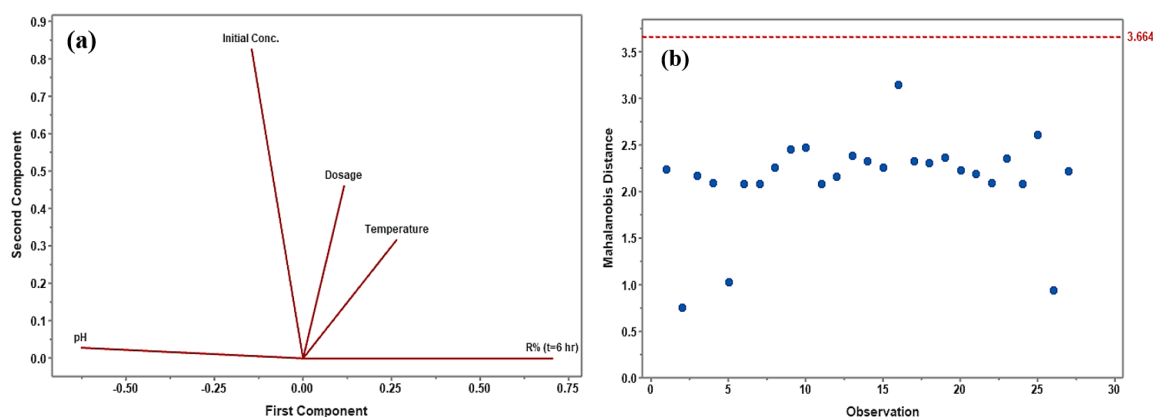


**Figure 4.** (a) Loading plots and (b) Outlier plots for wavelength of 230 nm.

Based on **Table 7**, the first principal component (PC 1) was strongly correlated with pH and aniline R% based on the distribution of each variable. PC 1 was interpreted as when the pH value decreased, it resulted in an increase of aniline R%. For the second principal component (PC 2), it correlated with the initial concentration of aniline only as the variable possessed the largest value among all the other variables. Nonetheless, the R% was 0 in PC 2 where it showed that the initial concentration of aniline has little impact on the aniline removal. Similar scenario happened to PC 3, where the medium temperature was the dominant variable for PC 3 and the R% has zero contribution percentage as well. Hence, a deviation in the medium temperature has little impact towards the aniline removal.

Outlier plot was plotted to determine outliers by referring to the reference line in the plot. Any point lied above the reference line was regarded as an outlier and it has significant impact towards the analysis results. According to the outlier plot in **Figure 4 (b)**, there were no outlier from the data points as all the points were below the reference line. Therefore, no correction was needed as all the data points were regarded as significant in the analysis.

#### **4. Conclusion**

The aniline adsorption performance of fresh graphite was systematically investigated. According to ANOVA analysis, pH was determined to be the most significant parameter that possessed a percentage contribution of 60.74%. Moreover, confirmation of studies was conducted to evaluate the reliability of the regression model generated from Minitab and the model was accepted as the deviation between the predicted value and experimental value was negligible. PCA supported that pH of aniline solution was the most significant factor in aniline adsorption process which the medium temperature was revealed as the least significant parameter.

#### **Acknowledgement**

This research work was funded by School of Engineering and Physical Sciences, Heriot-Watt University Malaysia.

#### **Credit Author Statement**

Conceptualization, Voon-Loong Wong and Swee Pin Yeap; methodology, Voon-Loong Wong and Chuan Xian Tan; software, Chuan Xian Tan; validation, Chuan Xian Tan; formal analysis, Chuan-Xian Tan; investigation, Chuan Xian Tan; resources, Chuan Xian Tan; data curation, Chuan Xian Tan; writing—original draft preparation Chuan Xian Tan; writing—review and editing, Siew Shee Lim, Sue Jiun Phang, and Voon-Loong Wong; visualization, Chuan Xian

Tan; supervision, Voon-Loong Wong and Swee Pin Yeap; project administration and funding acquisition, Voon-Loong Wong.

### Conflicts of Interest

The authors declare that they have no known competing financial interests or personal relationships that could have appeared to influence the work reported in this paper.

### References

- Annadurai, G., & Sheeja, R. (1998). Use of Box-Behnken Design of Experiments for the Adsorption of Verofix Red using Biopolymer. *Bioprocess Engineering*, 18, pp.463-466.
- Anotai, J., Su, C.-C., Tsai, Y.-C., & Lu, M. C. (2010). Effect of hydrogen peroxide on aniline oxidation by electro-Fenton and fluidized-bed Fenton processes. *Journal of Hazardous Material*, 183(1-3), pp.888-893.
- Anotai, J., Su, C.-C., Tsai, Y.-C., & Lu, M.-C. (2011). Comparison of Aniline Oxidation by Electro-Fenton and Fluidized-Bed Fenton Processes. *Journal of Environmental Engineering*, 137(5).
- Brereton, R. (2018). ANOVA tables and statistical significance of models. *Journal of Chemometrics*, 33(3).
- Cai, J., Li, A., Shi, H., Fei, Z., Long, C., & Zhang, Q. (2005). Adsorption characteristics of aniline and 4-methylaniline onto bifunctional polymeric adsorbent modified by sulfonic groups. *J Hazard Mater*, 124(1-3), pp.173-180.
- Chen, Y., Wang, B., Wang, X., Xie, L.-H., Li, J., Xie, Y., & Li, J.-R. (2017). A Copper(II)-Paddlewheel Metal-Organic Framework with Exceptional Hydrolytic Stability and Selective Adsorption and Detection Ability of Aniline in Water. *ACS Appl. Mater. Interfaces*, 9(32), pp.27027-27035.
- Dastkhon, M., Ghaedi, M., Asfaram, A., Goudarzi, A., & Mohammadi, S. (2017). Improved Adsorption Performance of Nanostructured Composite by Ultrasonic Wave: Optimization through Response Surface Methodology, Isotherm and Kinetic Studies. *Ultrasonics Sonochemistry*, 37, pp.94-105.
- Deng, Q., Chen, C., & Lei, Q. (2018). Adsorption of aniline from aqueous solution using graphene oxide-modified attapulgite composites. *RSC Advance*, 8, pp.23382-23389.
- Dutta, A. K. (1958). Characteristics of free electrons in graphite from a study of its magnetic and other properties. *Physica*, 24(1-5), pp.343-346.
- Coban, E. P., Biyik, H. H., & Saglam, U. C. (2020). Use of nanocellulose and microcellulose for aniline blue dye removal. *Fresenius Environmental Bulletin*, 29(11), pp.9542-9549.

- Gengec, N. A., Isgoren, M., Kobya, M., Veli, S., & Gengec, E. (2017). Optimization of Beidellite/Polyaniline Production Conditions by Central Composite Design for Removal of Acid Yellow 194. *Journal of Polymers and the Environment*.
- Greaves, R. (1992). Gibbs Free Energy The Criteria for Spontaneity. *Journal of Chemical Education*, 69(5), pp.417-418.
- Markit, I. H. S. (2016). Chemical economics handbook. Retrieved January, 3, pp.2022.
- Jaadi, Z. (2021). *A Step-by-Step Explanation of Principal Component Analysis (PCA)*. Retrieved November 23, 2021, from <https://builtin.com/data-science/step-step-explanation-principal-component-analysis>
- Jiang, Y., Wang, H., Yu, S., & Yang, K. (2016). Simultaneous removal of aniline, nitrogen and phosphorus in aniline-containing wastewater treatment by using sequencing batch reactor. *Bioresource Technology*, 207, pp.422-429.
- Jin, Y.-L., Lee, W.-N. L.-H., Chang, I.-S., Huang, X., & Swaminathan, T. (2006). Effect of DO concentration on biofilm structure and membrane filterability in submerged membrane bioreactor. *Water Research*, 40(15), pp.2829-2836.
- Leffler, J. (1955). The Enthalpy-Entropy Relationship and its Implications for Organic Chemistry. *The Journal of Organic Chemistry*, 20(9), pp.1202-1231.
- Li, X., Xu, H., & Yan, W. (2016). Electrochemical oxidation of aniline by a novel Ti/TiO<sub>x</sub>Hy/Sb-SnO<sub>2</sub> electrode. *Chinese Journal of Catalysis*, 37(11), pp.1860-1870.
- Liu, Q., Zhang, L., & Huang, R. (2015). Removal of aniline from aqueous solutions by activated carbon coated by chitosan. *Journal of Water Reuse and Desalination*, 5(4), pp.610-618.
- Liu, X., Xu, X., Sun, J., Alsaedi, A., Hayat, T., . . . Wang, X. (2018). Insight into the impact of interaction between attapulgite and graphene oxide on the adsorption of U(VI). *Chemical Engineering Journal*, 343, pp.217-224.
- Mah, C. Y., Azhar, N. N., Wong, V. L., Chen, Y. L., Yagoub, S. A. M., Teo, S. S., ... & Yeap, S. P. (2023). Loose and Encased Graphite for Methylene Blue Adsorption: Process Optimization and Principal Component Analysis. *Chemical Engineering & Technology*.
- Mohamed A., A.-R., Mohamed F., S., Safinaz H., E.-D., & Ahmed M., E.-N. (2020). Simulated kinetics of the atmospheric removal of aniline during daytime. *Chemosphere*, 255.
- Naga Babu, A., Krishna Mohan, G. V., Kalpana, K., & Ravindhranath, K. (2017). Removal of lead from water using calcium alginate beads doped with hydrazine sulphate-activated red mud as adsorbent. *Journal of Analytical Methods in Chemistry*.
- Nandiyanto, A., Oktiani, R., & Ragadhita, R. (2019). How to Read and Interpret FTIR Spectroscopy of Organic Material. *Indonesian Journal of Science & Technology*, 4(1), pp.97-118.

- Oetjik, W., & Ibrahim, S. (2021). A Review: The Effect of Initial Dye Concentration and Contact Time on The Process of Dye Adsorption using Agricultural Waste Adsorbent. *Progress in Engineering Application and Technology*, 2(2), pp.1051 - 1059.
- Padmavathy, K., Madhu, G., & Haseena, P. (2016). A study on effects of pH, adsorbent dosage, time, initial concentration and adsorption isotherm study for the removal of hexavalent chromium (Cr(VI)) from wastewater by magnetite nanoparticles. *Procedia Technology* 24, pp.585-594.
- Roosta, M., Ghaedi, M., Daneshfar, A., Sahraei, R., & Asghari, A. (2014). Optimization of the ultrasonic assisted removal of methylene blue by gold nanoparticles loaded on activated carbon using experimental design methodology. *Ultrasonics Sonochemistry*, 21(1), pp.242-252.
- Schneider, A., Hommel, G., & Blettner, M. (2010). Linear Regression Analysis. *PubMed Central*, pp.776-782.
- Smith, A. T., LaChance, A. M., Zeng, S., Liu, B., & Sun, L. (2019). Synthesis, properties, and applications of graphene oxide/reduced graphene oxide and their nanocomposites. *Nano Materials Science*, 1(1), pp.31-47.
- Verma, A., Thakur, S., Mamba, G., & Prateek. (2020). Graphite modified sodium alginate hydrogel composite for efficient removal of malachite green dye. *International Journal of Biological Macromolecules*, 148, pp.1130-1139.
- Wang, L., Barrington, S., & Kim, J.-W. (2007). Biodegradation of pentyl amine and aniline from petrochemical wastewater. *Journal of Environmental Management*, 83(2), pp.191-197.
- Wold, S., Esbensen, K., & Geladi, P. (1987). Principal Component Analysis. *Chemometrics and Intelligent Laboratory Systems*, 2(1-3), pp.37-52.
- Wong, K., Wong, V., & Lim, S. (2021). Bio-sorptive Removal of Methyl Orange by Micro-Grooved Chitosan (GCS) Beads: Optimization of Process Variables Using Taguchi L9 Orthogonal Array. *Journal of Polymers and the Environment*, 29, pp.271-290.
- Xiao, W., Zhou, P., Mao, X., & Wang, D. (2015). Ultrahigh aniline-removal capacity of hierarchically structured layered manganese oxides: trapping aniline between interlayers. *Journal of Materials Chemistry A*, 3(16), pp.8676-8682.